NASA CONTRACTOR
REPORT

NASA CR-150906

EVALUATION OF SHUTTLE TURBOPUMP BEARINGS

By K. D. Dufrane and J. W. Kannel
Battelle Columbus Laboratories
505 King Avenue
Columbus, Ohio 43201

Final Report

November 22, 1978

Prepared for

NASA-George C. Marshall Space Flight Center
Marshall Space Flight Center, Alabama 35812

TABLE OF CONTENTS

FINAL REPORT

on

EVALUATION OF SHUTTLE TURBOPUMP BEARINGS

to

GEORGE C. MARSHALL SPACE FLIGHT CENTER

from

BATTELLE
Columbus Laboratories

by

K. F Dufrane and J. W. Kannel

November 22, 1978

INTRODUCTION

NASA is currently involved in the development of long-life turbopumps for use on the shuttle. Because of the re-usable design of the shuttle, lifetimes of 27,000 seconds (7.5 hours) are being sought, whereas most turbopumps to date have operated for periods of on the order of only hundreds of seconds. While all components are being considered in efforts to achieve satisfactory lifetimes, the mainshaft support bearings are of particular concern. In support of these efforts, Battelle's Columbus Laboratories (BCL) undertook a one-month study to examine a used set of bearings and to recommend the subsequent steps needed to achieve the desired lifetimes.

The four bearings examined were run in a liquid oxygen turbopump on engine No. 2002. A total of 1758 seconds of running were accumulated, including 1452 seconds at 100 percent output (approximately 28,000 rpm). The bearings are angular-contact ball bearings, applied as preloaded pairs, locked to the shaft, inner race rotating, with the outer races unrestrained axially (i.e., the bearings provide radial location only). The bearings examined in the study and their locations were as follows:

Bearing Position	Bearing Serial Number	Bearing Part Number
1 (Pump End)	8492674	02602-5DRS007522-001
2	8492669	02602-5DRS007522-001
3	8517901	02602-2DRS007955-001
4 (Turbine End)	8517898	02602-2DRS007955-001

Battelle's specific objectives in the study were:

(1) Perform a visual, scanning electron microscopy (SEM), metallurgical, and dimensional analysis of the bearings (as needed).

(2) Estimate the nature and magnitude of the loads applied to the bearings based on the contact patterns.

(3) Recommend further analytical efforts required (including an estimate of magnitude of costs) and any design, material, or lubrication changes that will improve the durability of the bearings.

SUMMARY AND RECOMMENDATIONS

The most significant problems revealed by the bearing inspection were strong evidence of a high synchronous (unbalance) radial load and of debris indentations caused by foreign material passing through the bearings during operation. Foreign-debris denting is undesirable because the roughened surfaces contribute to rough bearing operation and interfere with generation of lubricant films between the balls and races during operation. Reduction of the denting requires a reduction in the quantity of foreign debris in the liquids passing through the bearings.

The large unbalance is significant because of the high resulting dynamic contact stresses generated on the bearing races. Based on predictions from a computer model and on actual measurements of the location of ball contact paths on the bearings, maximum radial unbalance loads of at least 10,000 Newtons (2200 pounds) were estimated. Such loads produce maximum

contact stresses at 2.8 GPa (410 ksi), which are extremely high for reliable bearing operation. Bearings having ball-race contact stresses at this high level are likely to fail by mechanisms such as wear and retainer failure as well as by contact fatigue. The predicted service life based solely on contact fatigue using a 90 percent survival (L_{10}) was calculated to be 8.8 hours, while the life at 99 percent survival (L_1) was only 1.1 hours. These life predictions are very short by normal bearing engineering standards. Furthermore, the data on which they were based were generated under ideal conditions of cleanliness, alignment, and liquid lubrication. Since the turbopump bearings operate in the presence of debris and with transfer-film lubrication, the expected fatigue life would be considerably less than the short times calculated under ideal conditions. The short predicted fatigue lives are a direct result of the high contact stresses and are significant only in that they indicate operation under conditions of intolerably high loading. For example, reducing the unbalanced radial load to zero extends the L_{10} fatigue life estimate to 1200 hours and the L_1 life to 145 hours. Calculated fatigue lives of this order are more reasonable for the turbopump application.

Based on the results of this effort, the following specific recommendations were made. The cost estimates for the efforts that might be appropriately performed at Battelle are provided in compliance with the contract requirements for planning purposes only. Battelle would submit a proposal and more accurate costs depending upon the exact requirements and our commitments at the time of the request.

(1) Conduct a critical review meeting with NASA, Rocketdyne, and Battelle technical personnel to discuss the results of the bearing analysis, their implications, and reasonable/possible areas for corrective design modifications. Assuming two Battelle staff members would attend, an expenditure of $4,000 to $5,000 would be required.

(2) Perform a similar inspection of at least one more set, and preferably two more sets, of used bearings from other turbopumps to provide additional data regarding the magnitude of the radial unbalance loads. The inspection of two more sets could be completed for an expenditure of $12,000 to $15,000.

(3) Conduct experiments to determine the contact-stress limitations of the TFE transferred to the bearing races. Since a threshold level has not been determined at Battelle for a similar lubricant,

the presence of a threshold for the TFE has serious implications for satisfactory bearing life under high radial load conditions. Alternate transfer-film lubricant types and MoS_2 dry-film coatings should also be considered. These efforts would require an expenditure of $20,000 to $30,000.

(4) Conduct a bearing dynamic analysis including the effects of cage loading. Transfer-film lubrication requires some cage loading for sufficient cage wear to occur. Further, cage instability is always of concern in bearings of this type. Performing a dynamic analysis would permit the needed understanding of the critical parameters to insure desirable operation. These efforts would involve an expenditure of $15,000 to $20,000.

(5) Investigate means for balancing the rotating members to reduce or eliminate the radial loads applied to the bearings. Since such efforts require a thorough knowledge of the turbopump design, they should probably be performed by Rocketdyne.

(6) Perform bearing life tests to reproduce the contact stress of 2.8 GPa (410 ksi) estimated in the bearings examined in this study. The results of these tests should help to define the seriousness of the fatigue and lubrication problem. If Rocketdyne has an existing test fixture for this purpose, it should be used for the tests. If their fixture is not appropriate, Battelle would discuss the possibility of constructing an appropiate fixture and conducting the needed tests. Cost estimates on such an effort would be prepared if needed.

BEARING INSPECTION

Visual and SEM

Races

The examination of the races revealed numerous debris indentations (dents) in all of the ball contact paths. The dents were caused both by relatively soft and hard debris. Soft debris dents formed early in the bearing life often display the original ground finish of the race at the bottom of the dent (which remains intact since it is not contacted further by the balls). The races of bearing 8517901 had several very large soft dirt dents displaying the original finish at the bottom of each. The inner race of this bearing also had a long thread-like indentation, which matched the appearance, size, shape, and length of the glass fibers observed to be loosely attached to the bearing separators. The contact paths on the other bearing races also displayed many round-bottomed indentations, but largely without finishing marks at the bottom. These were probably caused after the original finish had been obliterated by ball contacts.

All of the contact paths also had numerous indentations caused by hard debris. The dents were defined by angular sides often reaching sharp points at the bottoms of the depressions. Such dents are typically caused by minerals, such as SiO_2, or small carbides. The requirement is that the indenting material be harder than the bearing race. A typical area on the inner race of bearing 8492669 is shown in Figure 1. Numerous small debris dents are visible on the generally featureless ball contact path.

While the ball contact paths on the races were defined most clearly by the debris dents, they also showed wear through the depth of the original ground finish. However, since remnants of the deepest scratches were found in many of the contact paths (especially toward their edges), the maximum wear depth did not appear to be significantly deeper than the scratches.

A general brown film was observed on the race contact paths. This was assumed to be TFE transferred from the retainer. Islands of brown deposits forming continuous bands around the races were also located at the edges and occasionally at the centers of the contact paths. These were probably larger

2166 300X

FIGURE 1. SCANNING ELECTRON MICROSCOPE VIEW OF INNER RACE OF BEARING 8492669.

build-ups of TFE that had been forced out of the contact region during passage of the balls. Probing the deposits under the microscope showed them to be well attached to the race surfaces, but quite soft and easily scratched. A typical area of the deposits is shown in Figure 2 on the inner race of bearing 8492669.

Also of significance in the visual inspection was the location of the ball contact paths on the races. The contact paths on the inner races of bearings No. 3 and No. 4 (turbine end) had a significant ellipticity. In contrast, the contact paths on the outer races of these bearings were continuous in width and nonvarying in position. This combination is evidence of a significant synchronous radial load applied through the rotating inner races. The source of such a load is most likely to have been a dynamic imbalance of the shaft. Only the No. 2 bearing at the other end of the shaft showed no variation in the location of the inner race contact path. These observations provide evidence of a significant rotor imbalance primarily at the turbine end of this particular turbopump.

Balls

Inspection of the balls showed that they all had a tendency toward banding, which would be expected because of the significant axial load applied to angular-contact bearings. However, the bands were faint and on multiple axes. This indicates that the balls had been unloaded during portions of their orbit in the bearing or that the overall bearing loading had varied significantly during operation. The bands were defined mostly by debris dents of various sizes and a fine frosting of the original ball finish through wear. A typical area showing elongated dents on a ball form bearing 8517901 is shown on Figure 3a.

Most of the balls also had continuous small-circle scars on their surfaces, such as shown in Figure 3b. These are normally assumed to be caused by sliding contact with debris embedded in the retainer. If the balls continue to rotate about the same axis, such scars never contact the race, and therefore, are not of significance. However, when operating conditions change the axis of rotation, the scars can be placed in contact with the race and thereby contribute to torque variations (roughness). The flattened material at the edges of the scar in Figure 3b indicate that this portion of the ball had rolled through the race contact area after the scar was formed.

21165 300X

FIGURE 2. DEPOSITS AT EDGE OF BALL CONTACT PATH ON INNER RACE OF BEARING 8492669.

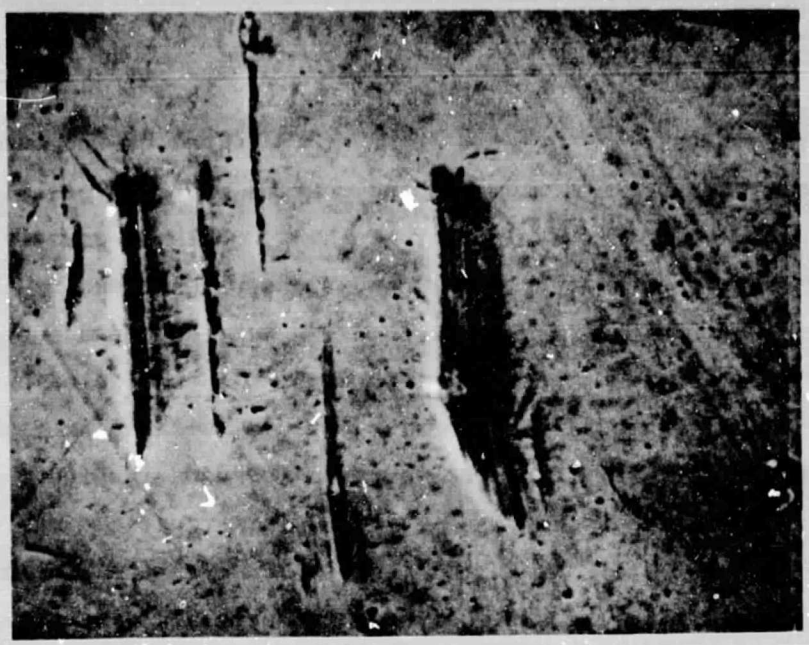

21157 1500X

a. Elongated Dents.

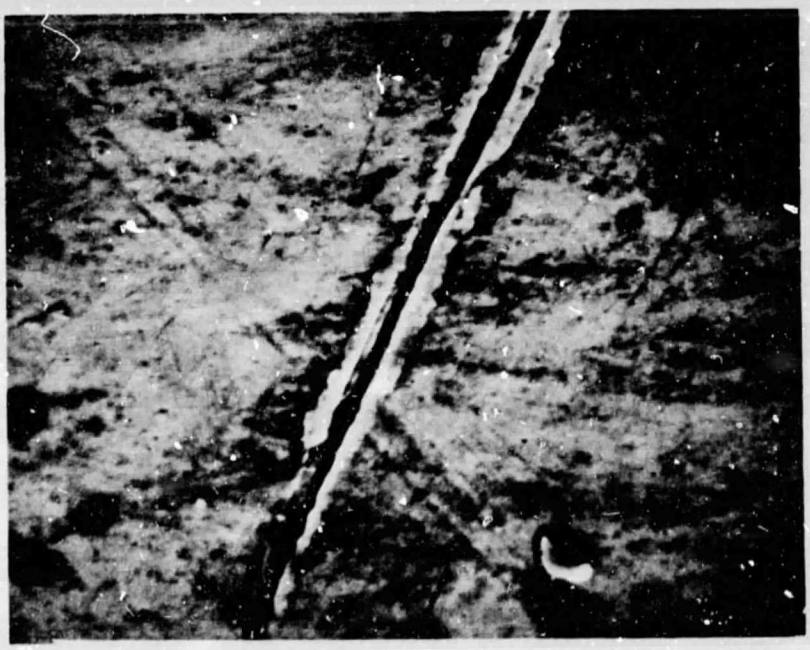

21158 1500X

b. Portion of Continuous Small-Circle Scar.

FIGURE 3. DAMAGED AREAS OBSERVED ON BALL FROM BEARING 8517901.

Retainers

The retainers all showed evidence of mild wear on the outer (guiding) surface and in the ball pockets from sliding contact with the balls. There was no evidence of heavy wear, distortion, or cracking, which is associated with high ball-retained loads developed under conditions of distress.

Several of the ball pockets and guiding surfaces had embedded metallic debris observable by low-power optical microscopy. An example of the debris observed in an SEM on the retainer of bearing 849674 is shown in Figure 4a. The X-ray fluorescence pattern of this area for iron is shown in Figure 4b, which identifies the metallic debris in Figure 4a. A similar pattern was developed for chromium, which suggests that the debris is most likely a steel alloy, such as the bearing race steel itself. Since some of the metallic particles protruded from the surfaces of the ball pockets, they may have been responsible for wear scars on the balls.

The rod-shaped particle in Figure 4a is a segment of the glass fiber reinforcing used in the retainer. A view of the fibers in another portion of a ball pocket on the retainer from bearing 8492674 is shown in Figure 5. The TFE is visible between the fibers and was often present as the loosely attached particles seen in Figure 5. Since the ball pockets are machined normal to the lay direction of the fibers, the intersection with the ends of the fibers is expected. On a microscale these present a rough surface for the balls and probably are responsible for the mild frosted appearance of the ball surfaces.

Talysurf Measurements

While the Talysurf profilometer cannot reliably measure profile changes over large curved areas without similar before-wear profiles for comparison, it is very useful in assessing the extent of local wear and the depth of indentations. Figure 6 presents traces across the inner race ball-contact areas of all four bearings. The general shapes of the curves are meaningless, but local dents or scratches can be seen ranging in depth from 0.5 μm (20 microinches) to nearly 2.0 μm (80 microinches). The buildup of soft debris on the inner race of bearing 8517901 is seen to have local peaks approximately 0.8 μm (30 microinches) high and a possible general buildup of 2.0 μm (80 microinches) (assuming the central raised area is all part of the deposit). The original surface finishes were probably similar to the uncontacted areas at the right end of the traces.

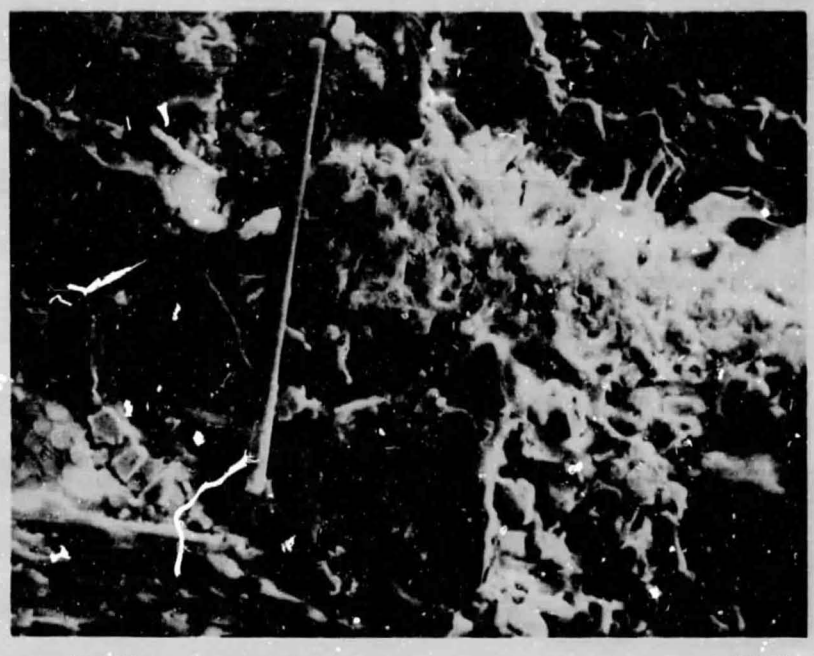

21161 500X

a. Debris.

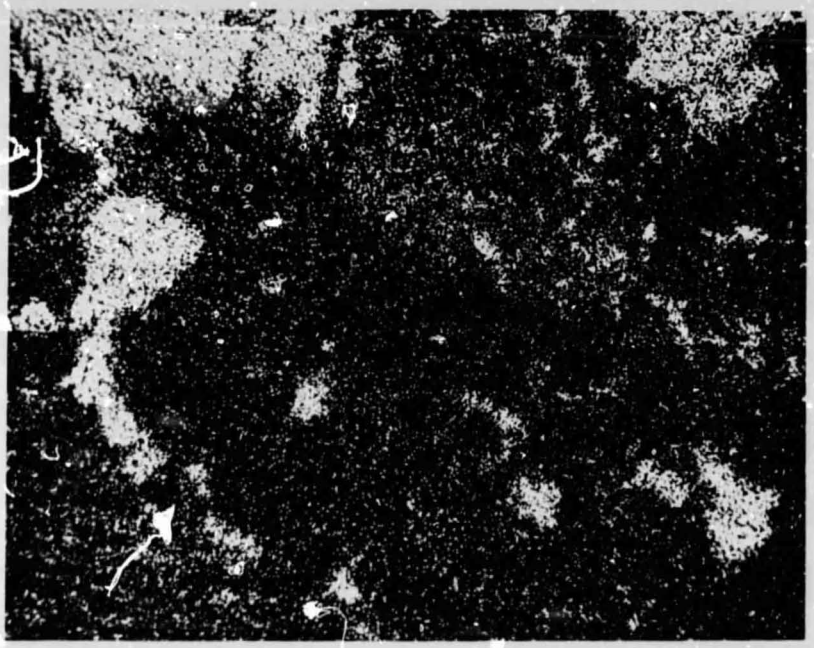

21160 500X

b. X-ray Scan for Iron.

FIGURE 4. SEM OBSERVATION OF METALLIC DEBRIS IN BALL POCKET OF 8492674 BEARING RETAINER.

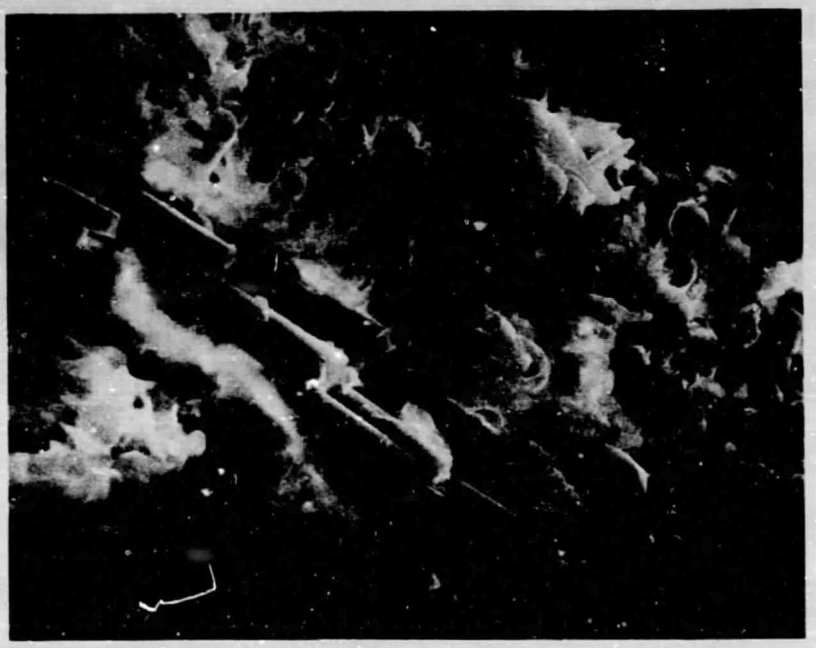

21159 1000X

FIGURE 5. ENDS OF GLASS FIBERS IN BALL POCKET OF SEPARATOR FROM BEARING 8492674.

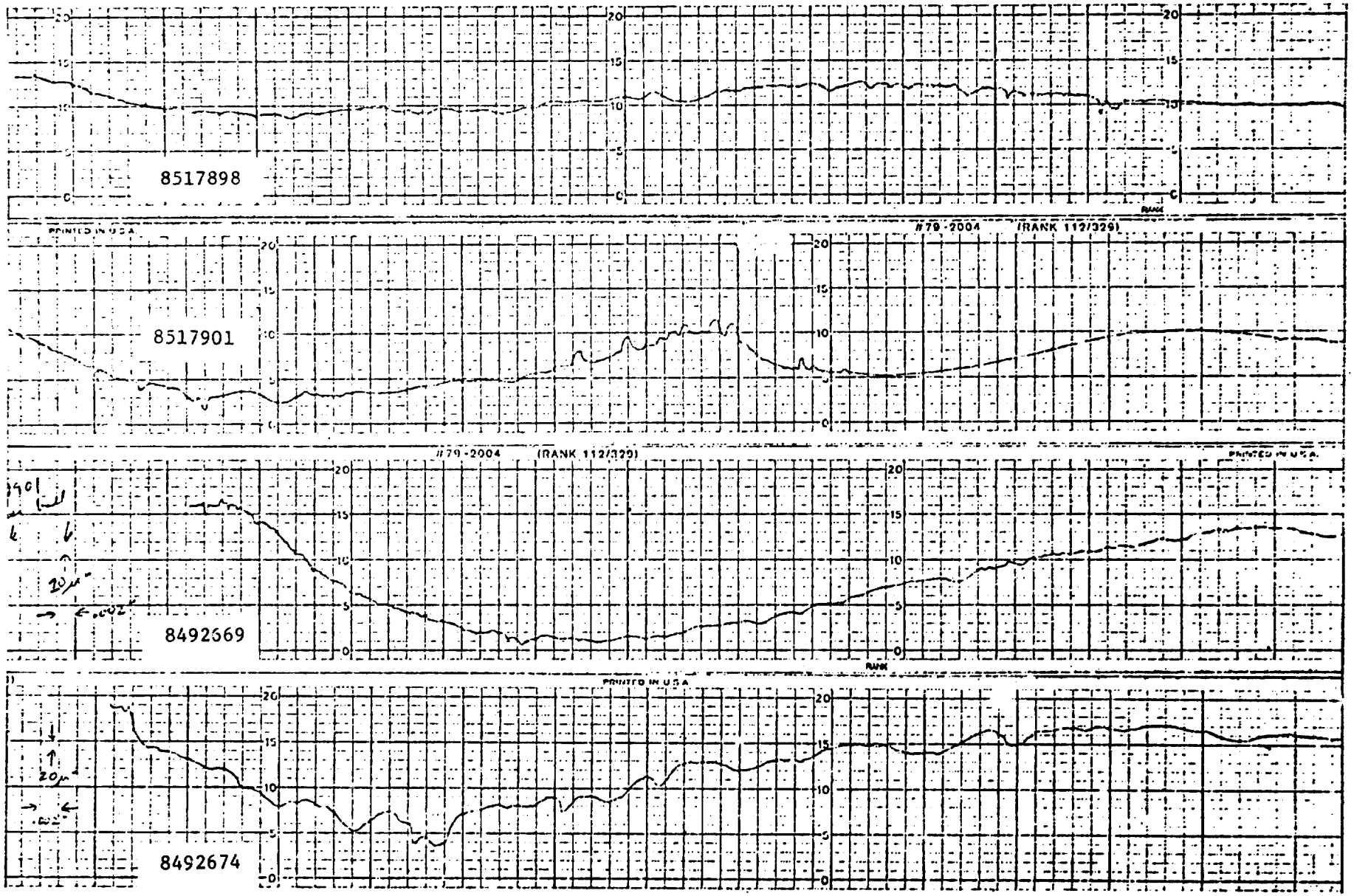

FIGURE 6. CURVE-MATCHING TRACES ACROSS BEARING INNER RACES. MAGNIFICATIONS, MINOR DIVISIONS,
VERTICAL: 0.05 μm (20 microinch)
HORIZONTAL: 0.05 mm (0.002 inch)

Figure 7a shows profiles of the minor-circle scratches on a ball from bearing 8517901. Scratch depths up to 1 μm (40 microinches) were measured. Although debris embedded in the ball pockets is generally assumed to cause such scratches, a second possible source may be the result of the sliding/rolling contact on the chamfer of the inner races during periods of very high inner-race contact angles. To explore this possibility, traces of the chamfer corners were made at the same magnification as was used on the balls, shown in Figure 7b and 7c. The radii at the tips of the chamfer corners are seen to match the radii of many of the ball scratches and could, therefore, have caused these scratches. The few scratches with sharper radii were caused by sliding against a sharper object, which was probably embedded debris.

In Figures 8 and 9, the Talysurf was used to measure the extent of retainer wear at the ball-and outer-race contact areas. In figure 8, ball pocket wear depths of approximately 23 to 38 μm (900 to 1500 microinches) were measured on the three retainers provided. The wear on the outer guiding surfaces was less, as seen in Figure 9. Only the peaks of the wrapped structure were worn off in the right portion of the trace where the retainer contacted the race. A wear depth of approximately 13 μm (500 microinches) was measured. Since the lubrication of the bearing is assumed to result from wear transfer of the TFE in the retainer, wear such as that measured is desirable.

Metallurgical Analysis

Metallurgical sections were prepared of a race from each bearing to examine the microstructure. A typical area of two bearings is shown in Figure 10. In Figure 10a, taken at the surface, a debris dent was intersected and is visible at the upper surface. The general microstructures are typical of 440C bearing steel, and no evidence of cracking, decarburization, retained austenite, or finishing damage was noted. Hardness readings taken on each of the races are presented in Table 1.

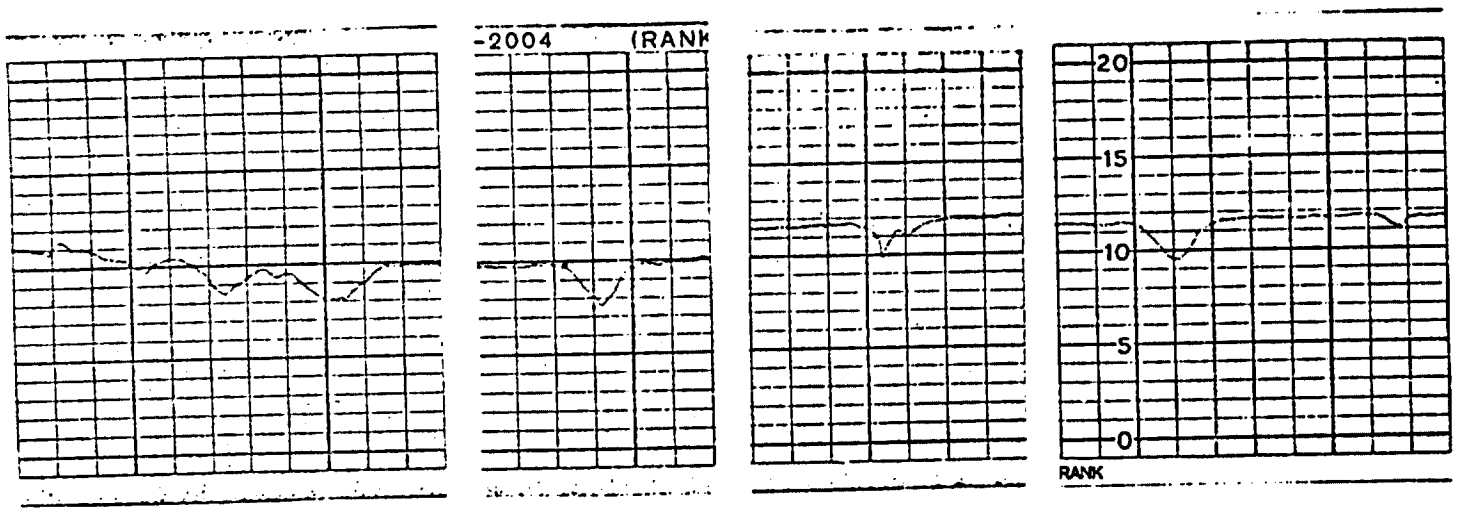

a. Scratches in Ball from Bearing 8517901.

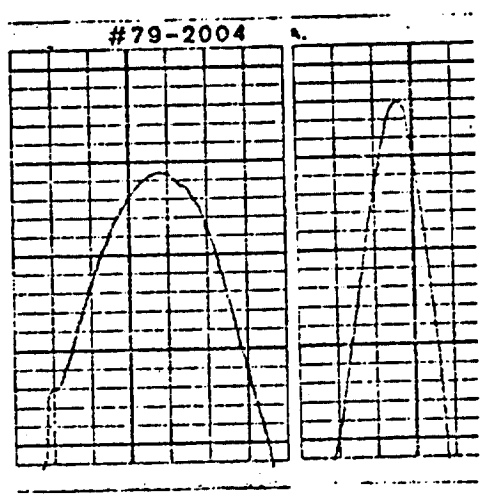

b. Chamfer Corners on Bearing 8517901.

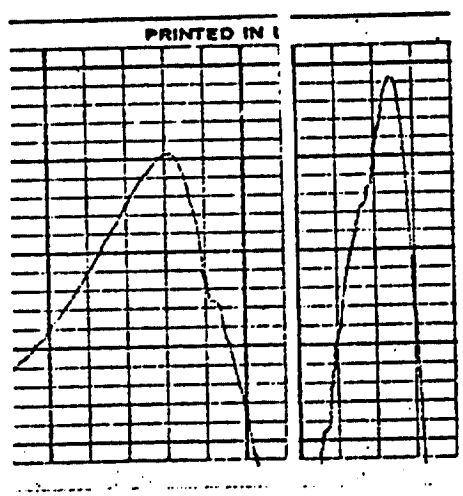

c. Chamfer Corners on Bearing 8492669.

FIGURE 7. PROFILES OF BALL SCRATCHES AND CORNERS OF INNER RACE CHAMFER. MAGNIFICATIONS, MINOR DIVISIONS, VERTICAL: 0.5 µm (20 microinch) HORIZONTAL: 0.005 mm (.002 inch)

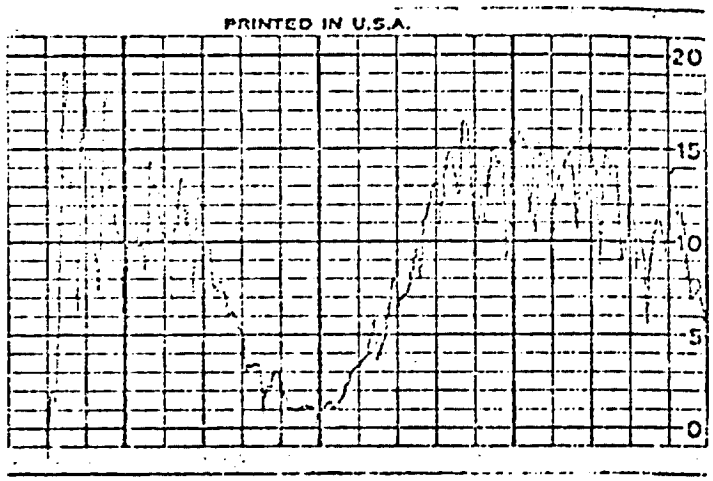

a. Bearing 8492674.

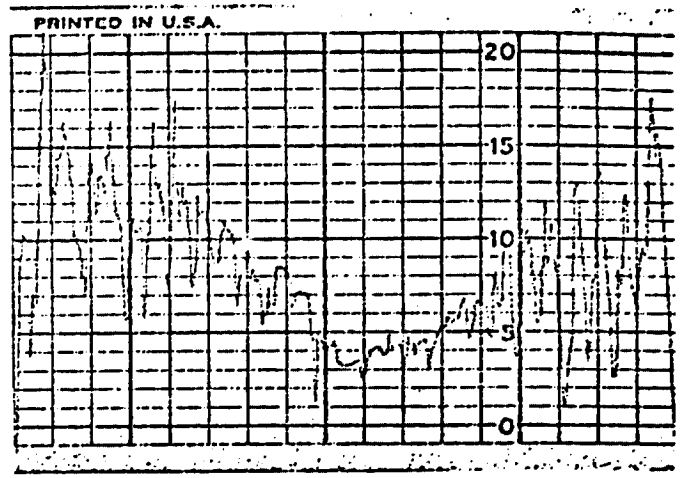

b. Bearing 8517901.

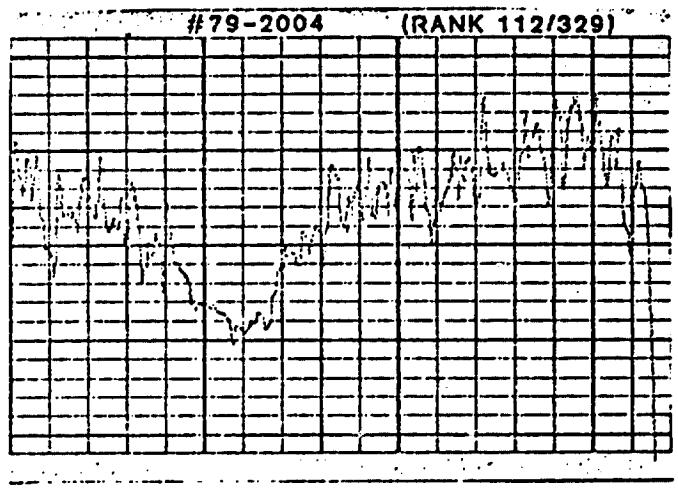

c. Bearing 8492669.

FIGURE 8. PROFILES OF MAXIMUM WEAR AREAS OF RETAINER BALL POCKETS.
MAGNIFICATIONS, MINOR DIVISIONS, VERTICAL: 2.5 µm (100 microinch)
HORIZONTAL: 0.25 mm (.010 inch)

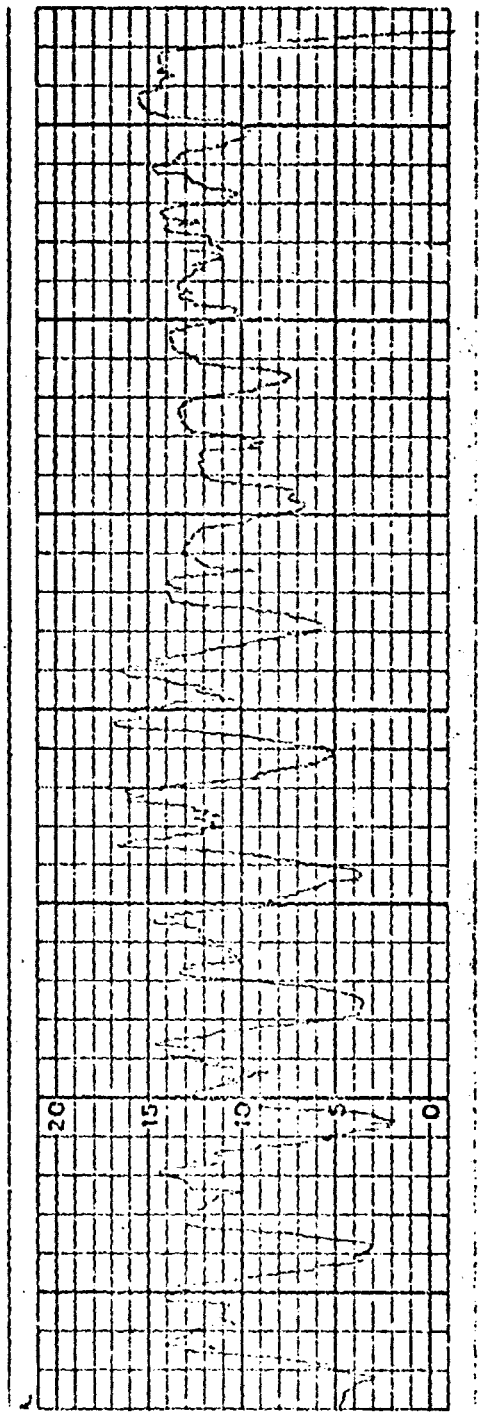

FIGURE 9. WEAR OF RETAINERS ON OUTER DIAMETER FROM SLIDING CONTACT WITH RACE.
MAGNIFICATIONS, MINOR DIVISIONS, VERTICAL: 2.5 μm (100 microinch)
HORIZONTAL: 0.25 mm (.010 inch)

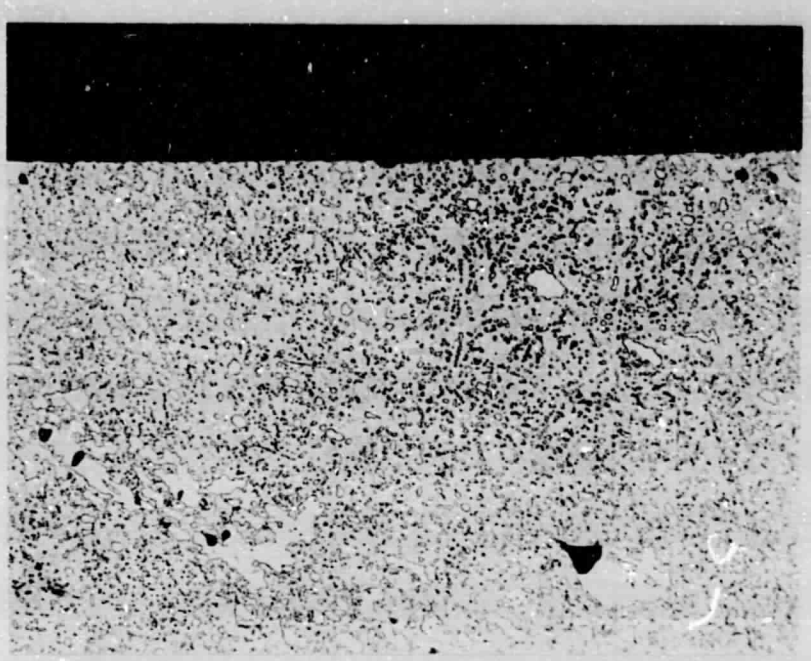

6J991 500X

a. Bearing 8492674 Inner Race, with Dent on Surface.

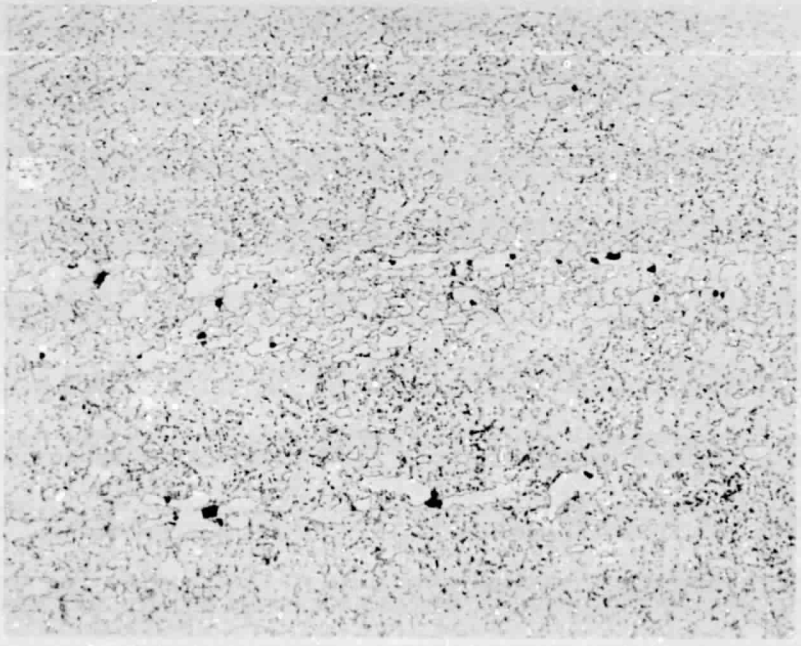

6J992 500X

b. Bearing 8492674 Outer Race.

FIGURE 10. TYPICAL BEARING STEEL MICROSTRUCTURE.

TABLE 1. ROCKWELL C HARDNESS READINGS OF BEARINGS RACES.

Bearing	R_C Hardness Inner Race	Outer Race
8492674	61	59
8492669	61	59
8517898	60	60
8517901	59	60

LOAD AND STRESS ANALYSIS

General Approach

The bearing inspections have shown not only that significant debris denting was present, but also that considerable variation occurred in the location of the ball contact path in the bearings. Such a variation is probably the result of radial loading due to imbalances in the shaft. The purposes of the load analyses have been to estimate the magnitude of the radial loads and the bearing stresses associated with these loads.

The method for bearing load computation at Battelle involves the use of a computer program series under the general name, BASDAP. BASDAP programs can be used for static or dynamic analysis of bearings for a wide range of applications. For example, BASDAP programs have been used in:

(1) Static or quasi-dynamic analyses to determine ball-race stresses and ball steady-state motions
(2) Determining the effects of unusual load conditions such as staggered ball spacings
(3) Analyses of dynamic behavior of the cage to determine cage stability and ball-cage loadings.

The BASDAP program treats each bearing, in a set, independently.

For the project discussed herein, only a quasi-dynamic version of BASDAP computer code was utilized. This code involves calculation of ball-race forces (inner and outer), contact pressures, contact dimensions, and contact angles as a function of:

(1) Axial load
(2) Radial load
(3) Centrifugal load

on the bearing.

The computation technique involves first computing the load sharing between the balls in the absence of centrifugal forces. This involves a formalized trial and error (nesting type) procedure. Essentially, estimates of the axial and radial deflection of the bearing are made. The correct value of these deflections result in the correct radial and axial load. After the ball load sharing has been computed, the effect of centrifugal force on contact angle is computed. Essentially, this force causes the inner and outer race

contact angles to be different from each other as well as different from the static contact angles. The method for the deflection and contact angles calculation is modeled after the classic work of A. B. Jones.*

Results of Calculations

The two bearing sizes (see Table 2) were analyzed in the calculations for two axial load conditions and several radial loads. Figures 11 and 12 show the effect of radial load on predicted contact angle. Notice in Figure 12, for example, that the outer race contact angle is relatively insensitive to radial load above about 3000N, while variation by as much as 6-7 degrees occurs on the inner race.

Figures 13 and 14 show the variation of Hertz half width with radial load. As the load is increased, the half width increases due to the increased ball-to-race loading. Figures 15 and 16 show the effect of radial load on maximum Hertz stress. At radial loads above about 2000N (440 lbs), the Hertz stress exceeds 2 GPa (28000 psi) which (as will be discussed in a following section) is extremely high for transfer film lubrication.

Estimation of Actual Radial Loads

Measurements were made of the location and width of the ball contact paths on the pump bearing races supplied by NASA, by using an optical microscope. The results are shown in Table 3. Using these measurements and the graphs presented in Figures 11 through 14, an estimation was made of the maximum radial load applied to each bearing race. Axial loads were assumed of 2900N (650 lbs) on the type 7522 bearings and 3800N (850 lbs) on the type 7955 bearings. An example of the procedure is shown in Figure 17, which is based on a scale drawing of the bearing races in their nominal position during operation. By graphical iteration, the load was chosen for each race that gave the best simultaneous fit of contact angle and Hertz half width for the extreme edge of the ball contact path (maximum radial load position). The maximum radial loads obtained for each bearing race are presented in Table 3.

With the estimation of maximum radial load, the graphs in Figures 15 and 16 were used to estimate the maximum ball-race contact stress. These

* Jones, A.B., "A General Theory for Elastically Constrained Ball and Roller Bearings under Auxiliary Load and Speed Conditions, Trans. ASME, J. Basic Eng., Vol. 82, Ser D., No. 2, June 1960, pp. 309-320.

are also included in Table 3. These estimations show that the contact stresses resulting from the large radial (unbalance) loads are very high by normal bearing engineering standards. These will be discussed further in a following section concerning life predictions.

TABLE 2. ASSUMED BEARING DESIGN CONDITIONS

Parameter	Units	Bearing Type 7955	Bearing Type 7522
Ball Diameter	m(in)	.012 (.500)	.011 (.4375)
Pitch Diameter	m(in)	.081 (3.19)	.065 (2.56)
Contact Angle	Degrees	20.5	24.5
Inner Race Curvature		.53	.53
Outer Race Curvature		.53	.52
Number of Balls		13	13
Speed	RPM	30000	30000

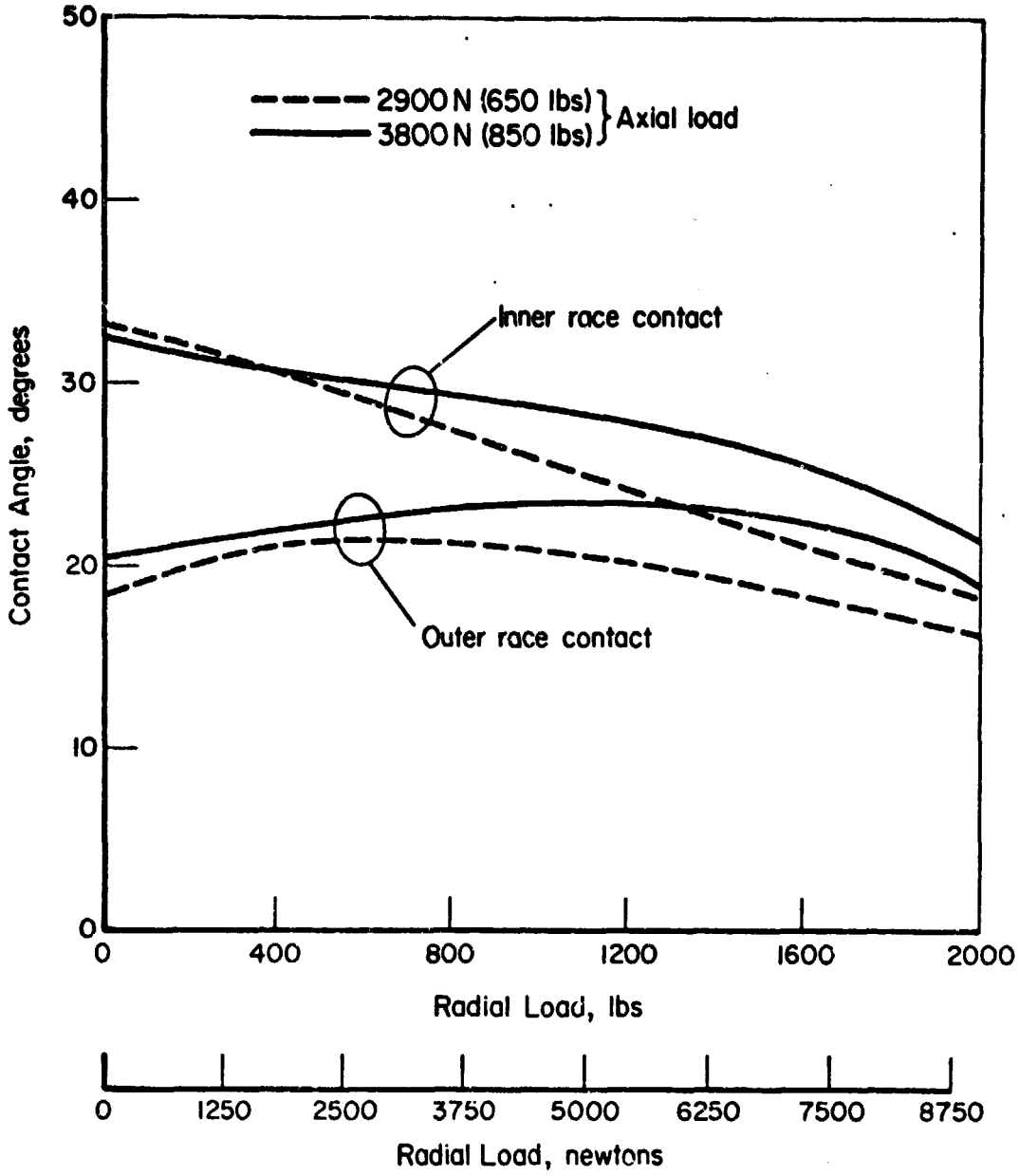

FIGURE 11. EFFECT OF RADIAL LOAD ON OPERATING CONTACT ANGLE, BEARING TYPE 7522.

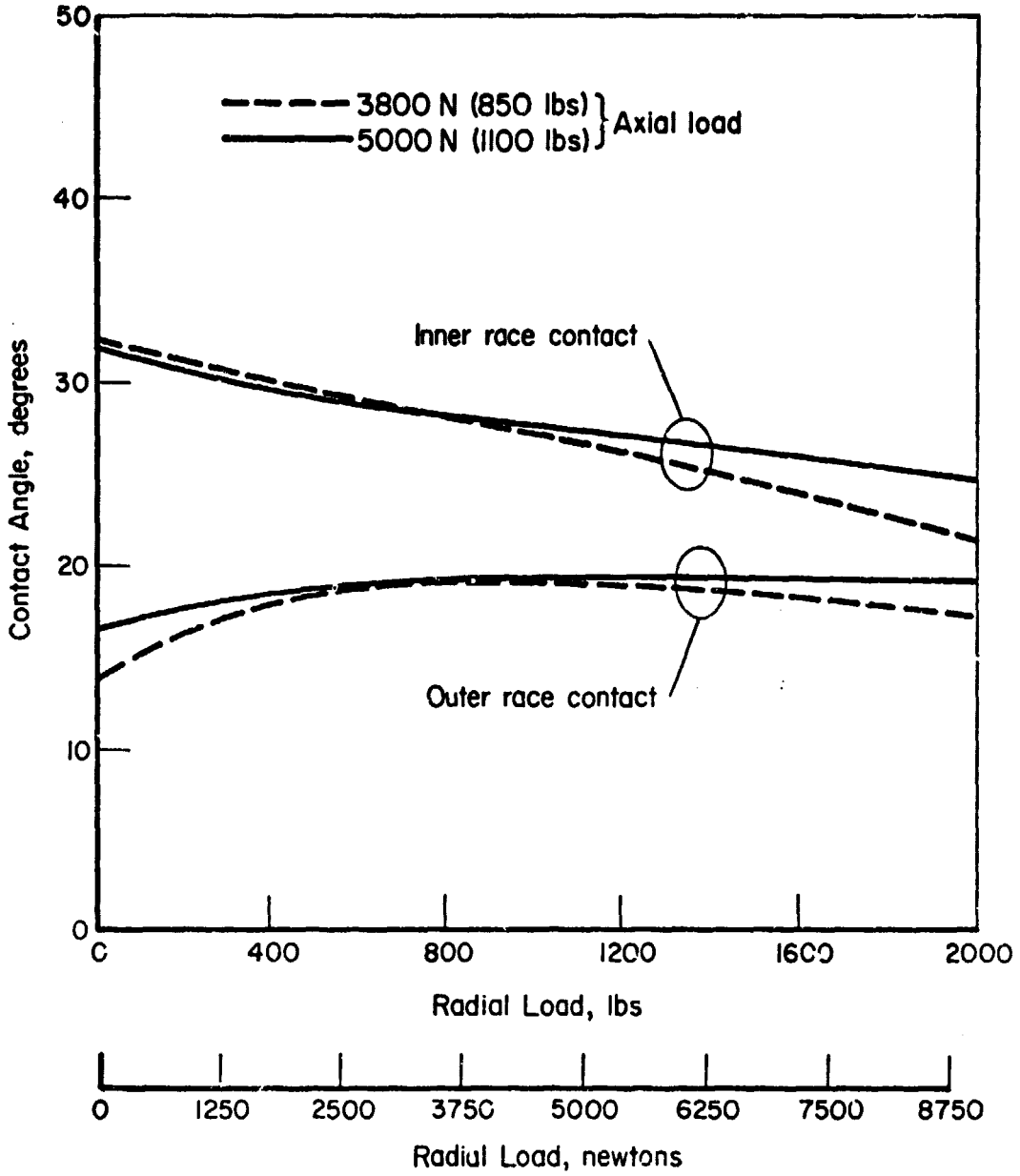

FIGURE 12. EFFECT OF RADIAL LOAD ON OPERATING CONTACT ANGLE, BEARING TYPE 7955.

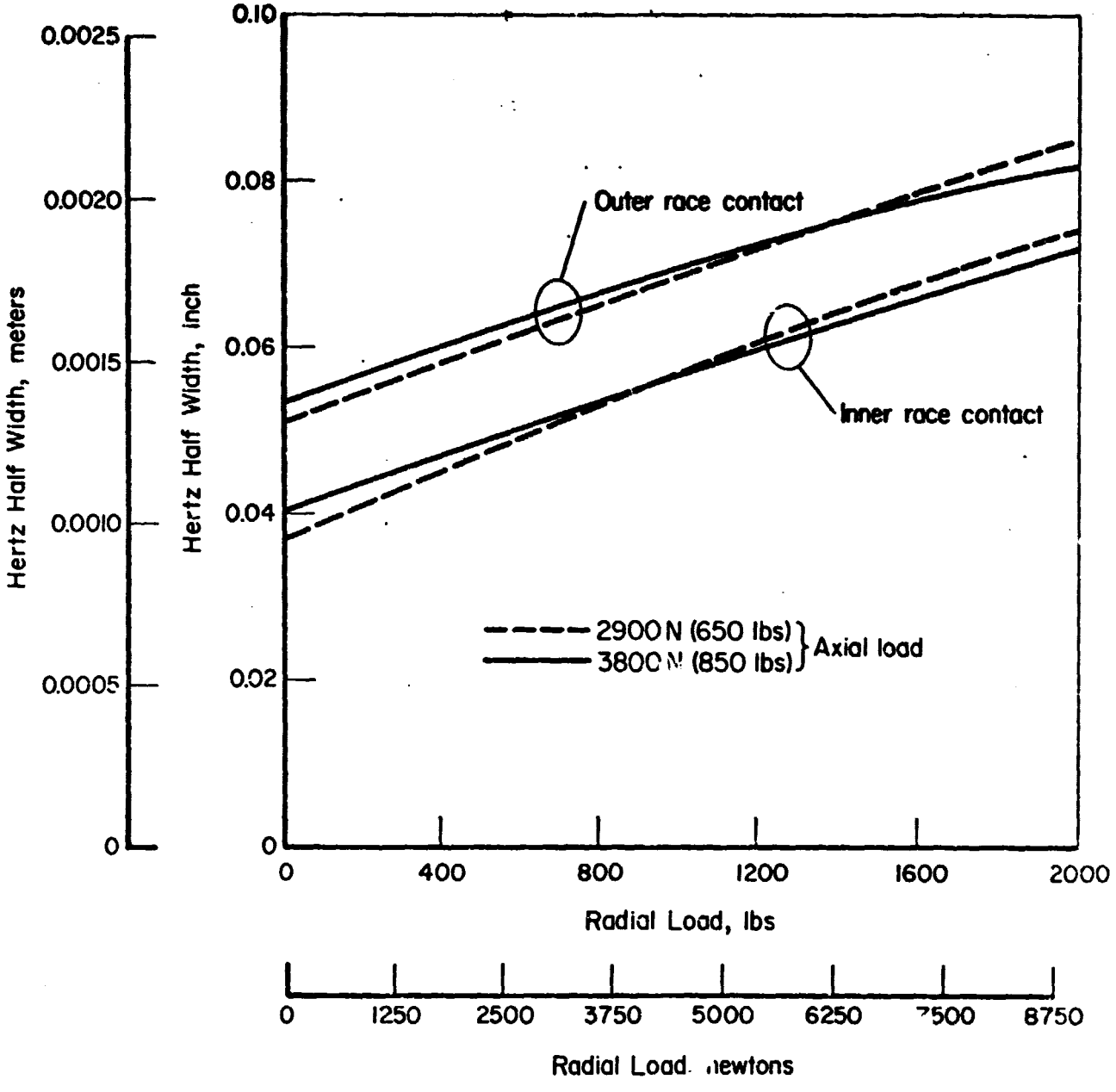

FIGURE 13. EFFECT OF RADIAL LOAD ON HERTZ CONTACT WIDTH, BEARING TYPE 7522.

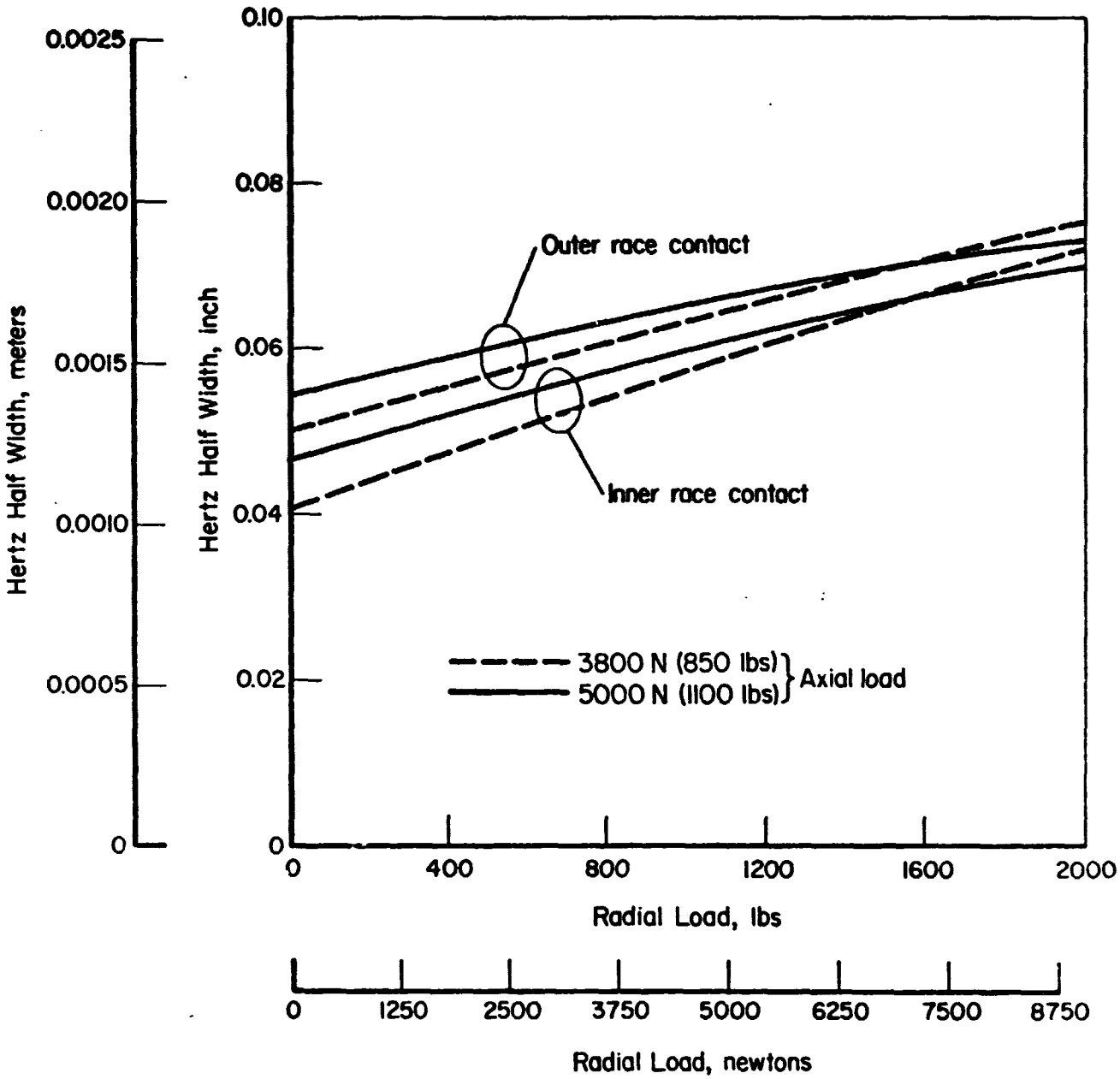

FIGURE 14, EFFECT OF RADIAL LOAD ON HERTZ CONTACT WIDTH, BEARING TYPE 7955.

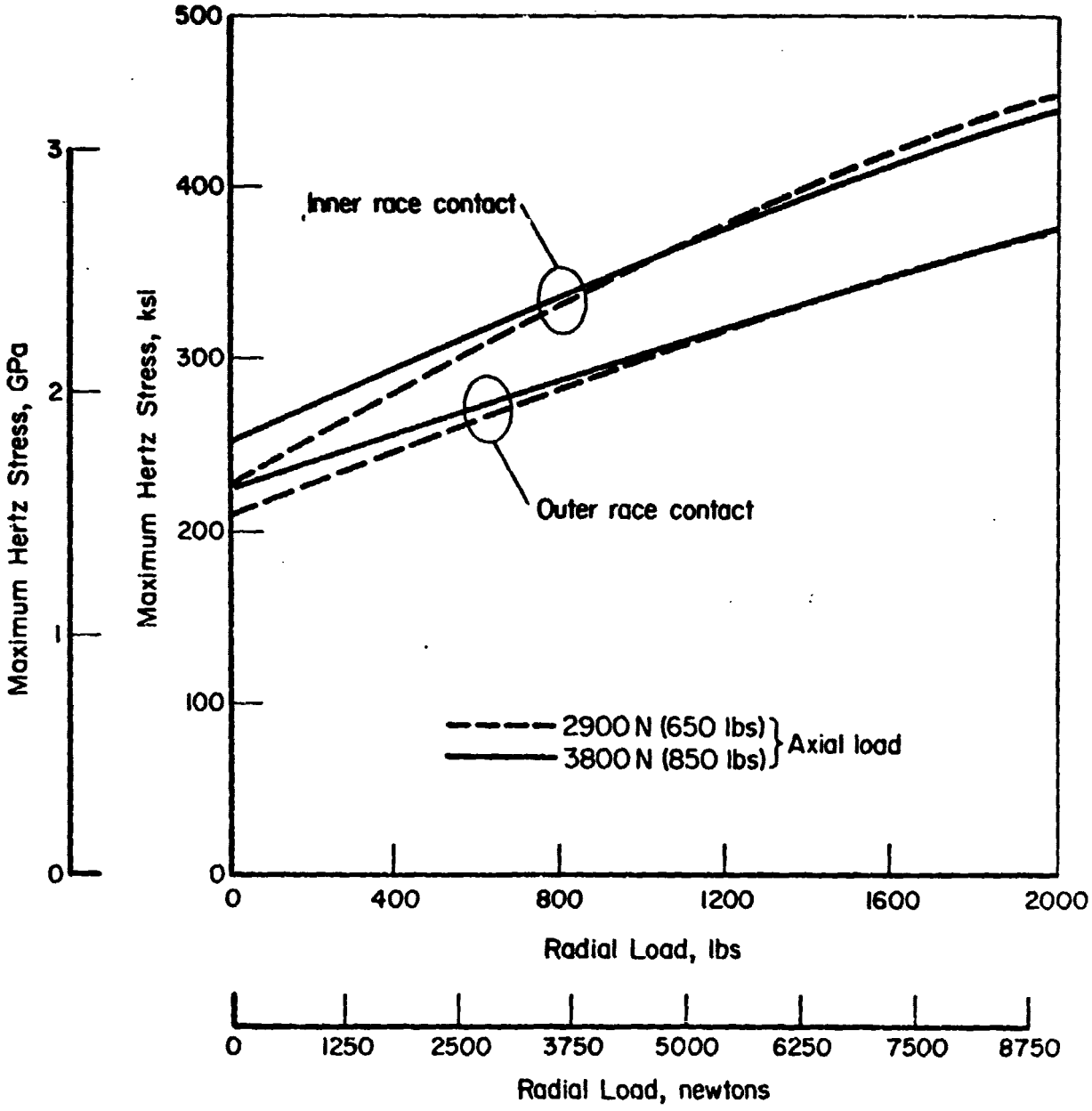

FIGURE 15. EFFECT OF RADIAL LOAD ON HERTZ CONTACT STRESS, BEARING TYPE 7522.

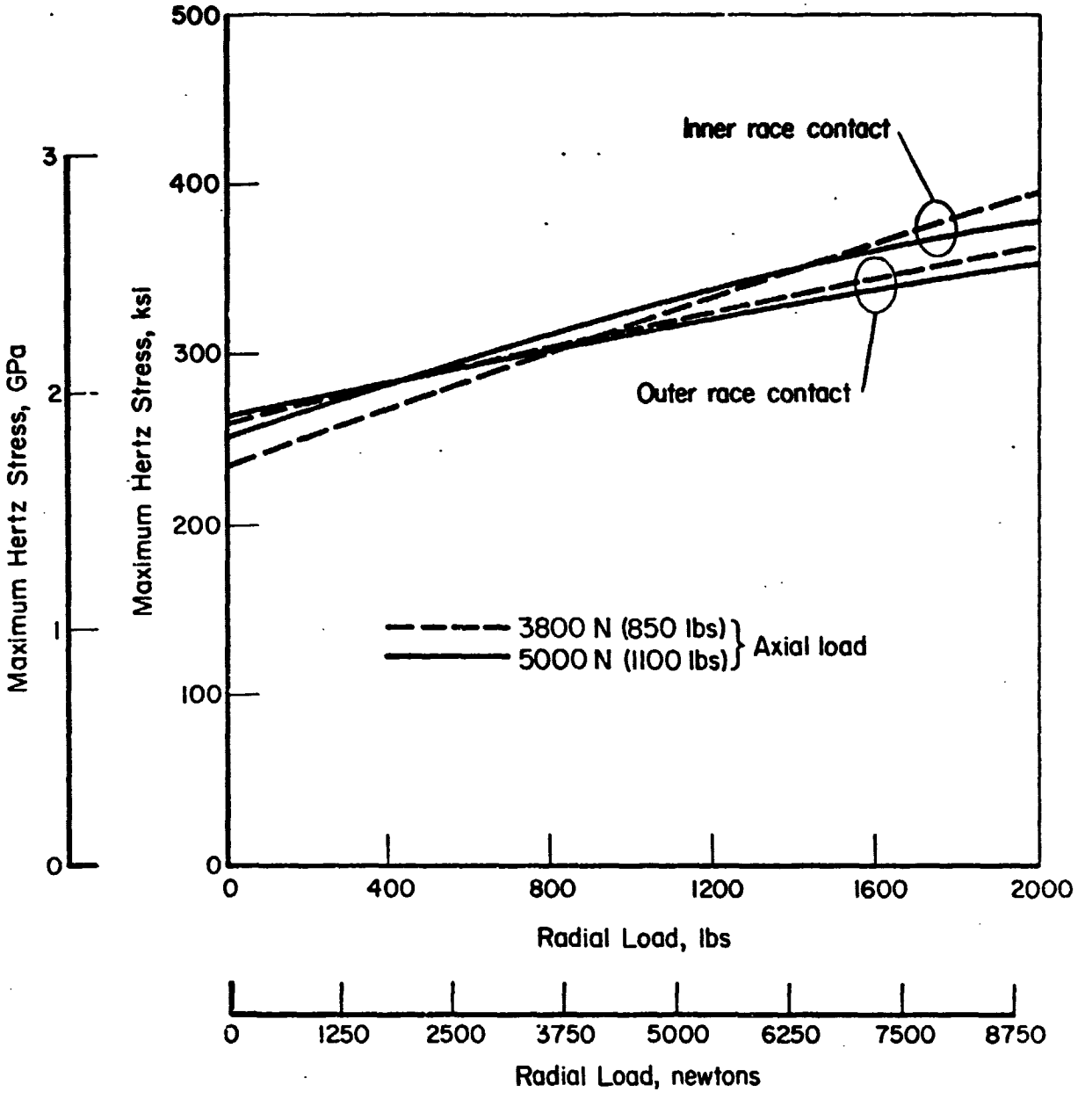

FIGURE 16. EFFECT OF RADIAL LOAD ON HERTZ CONTACT STRESS, BEARING TYPE 7955.

TABLE 3. WIDTHS AND LOCATIONS OF BALL CONTACT PATHS

Bearing	Inner Race				Outer Race			
	Measured Track Width, Meters (inches)	Measured Corresponding Distance From Race Edge, Meters (inches)	Maximum Estimated Radial Load, Newtons (pounds)	Maximum Estimated Contact Stress, GPa (KSI)	Measured Track Width, Meters (inches)	Measured Corresponding Distance From Race Edge, Meters (inches)	Maximum Estimated Radial Load, Newtons (pounds)	Maximum Estimated Contact Stress, GPa (KSI)
8492674 Type 7522)	.0025 (0.100)	.0013 (0.050)	2200 (500)	2.0 (290)	.0030 (0.118)	.0018 (0.072)	0 (0)	1.4 (210)
8492669 Type 7522)	.0031 to .0035 (0.123 to 0.136)	.0014 to .00094 (0.054 to 0.037)	3500 (800)	2.3 (330)	.0033 (0.130)	.0019 (0.073)	5300 (1200)	2.2 (320)
3517901 ype 7955)	.0043 to .0048 (0.170 to 0.189)	.0014 to .00046 (0.055 to 0.018)	10,000 (2200)	2.8 (410)	.0042 (0.165)	.0027 (0.107)	11,500 (2600)	2.8 (400)
517898 e 7955)	.0039 to .0043 (0.155 to 0.170)	.0020 to .00036 (0.080 to 0.014)	10,000 (2200)	2.8 (410)	.0035 (0.136)	.0029 (0.116)	10,000 (2200)	2.6 (370)

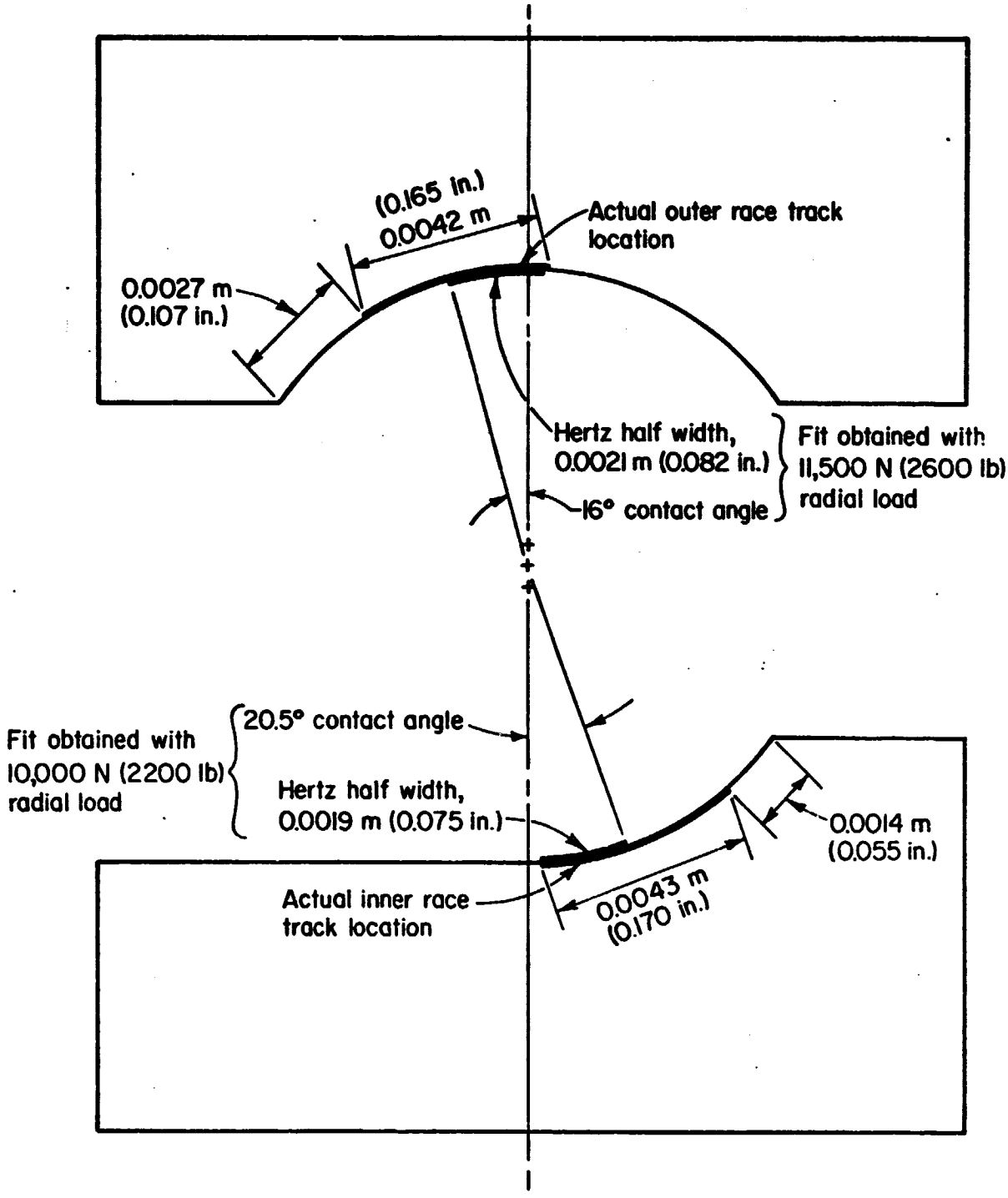

FIGURE 17. LOCATION OF ACTUAL BALL CONTACT PATHS ON BEARING 8517901 SHOWING FIT OF CONTACT ANGLES AND HERTZ HALF WIDTHS OBTAINED FROM FIGURES 12 and 14.

DISCUSSION

There are many possible reasons for a bearing to fail to perform its required function for an acceptable period of time. The two most common causes of failure are fatigue of the bearing steel and inadequate lubrication.

Fatigue Considerations

In 1947, Lumberg and Palmgren published a theory for the failure distribution of ball and roller bearings. This theory is summarized by Coy, et al. in NASA TND-8362 (Dec. 1976). Basically, the theory stated that bearing life can be expressed as

$$L_{10} = \left(\frac{K_1 z_o^h}{T_o^c V} \right)^{1/e} , \qquad (1)$$

where L_{10} = Life in millions of stress cycles (Based on 90% survival)

$K = 3.58 \times 10^{56}$ (based on 52100 steel, English units)

$e = 1.11$

$h = 2.334$

$c = 10.334$

V = stress volume ($z_o \ell w$)

w = semi-width of rolling track

z_o = depth of maximum shear stress

T_o = maximum shear stress

ℓ = length of rolling track.

Using the worst case postulated in Table 3, 9800N (2200 lbs) radial and 3800N (850 lbs) axial load on bearing 8517898,

$z_o = .037$ inches

$T_o = 123000$ psi

$\ell = 8.5$ inches (SI units)

$V = .024$ cubic inches

so

$L_{10} = 103$ million cycles

or 8.8 hours of bearing operation (assuming 6.5 stress cycles per revolution)

Based on a 99 percent survival, the life prediction is,

$L_1 = 12.8$ million cycles, or 1.1 hours.

This implies a marginal bearing fatigue life with this bearing which could easily result in very early failure of the bearings. Bearing life could also be considerably diminished by the surface dents which serve as initial failure points. This fatigue problem is largely the result of the high radial unbalance load. For example, if no radial load existed, the L_{10} life would be more like 1200 hours of bearing operation (L_1 life would be 145 hours) as a result of the axial load only.

Lubrication Effects

There are, of course, many assumptions inherent in a fatigue life estimate. For example, the fatigue life of 440C steel will be different from that of the 52100 steel. However, the most critical assumption regards the lubrication of the bearing. The fatigue theory was developed for liquid lubricated bearings where an adequate supply of lubricant is always available. In solid or transfer film lubrication conditions, the availability and adequacy of the lubricant is very much open to speculation. Surely, then, fatigue life with a solid film in this kind of application would be expected to be less than with normal lubricants.

One possible problem with solid film lubrication is in the stress limitation of the film itself. Battelle has conducted some experiments in other projects to characterize solid film strength. Figure 18 shows the result of one such series of tests. It should be noted that these tests were conducted for a different solid film and under much different conditions than being encountered in this project. However, the trends shown in these data are very critical. These data indicate that above a stress of 2 GPa (230,000 psi) solid film failure may occur (as noted previously, the estimated stress for the bearings investigated here was 2.8 GPa (410,000 psi).

In Table 3, it is obvious that if a high radial (unbalanced) load occurs, very high stresses will occur in the bearing. Not only can these high stresses greatly reduce classic fatigue life of the bearing but, in addition, it is possible (or even probable) that these stresses exceed the limit of the solid films. It is apparent, then, that tests to determine the limits of the film need to be established. It is also obvious that radial-unbalance loads must be minimized if adequate life of the bearing is to be achieved, both on the basis of the lubricant film as well as contact fatigue.

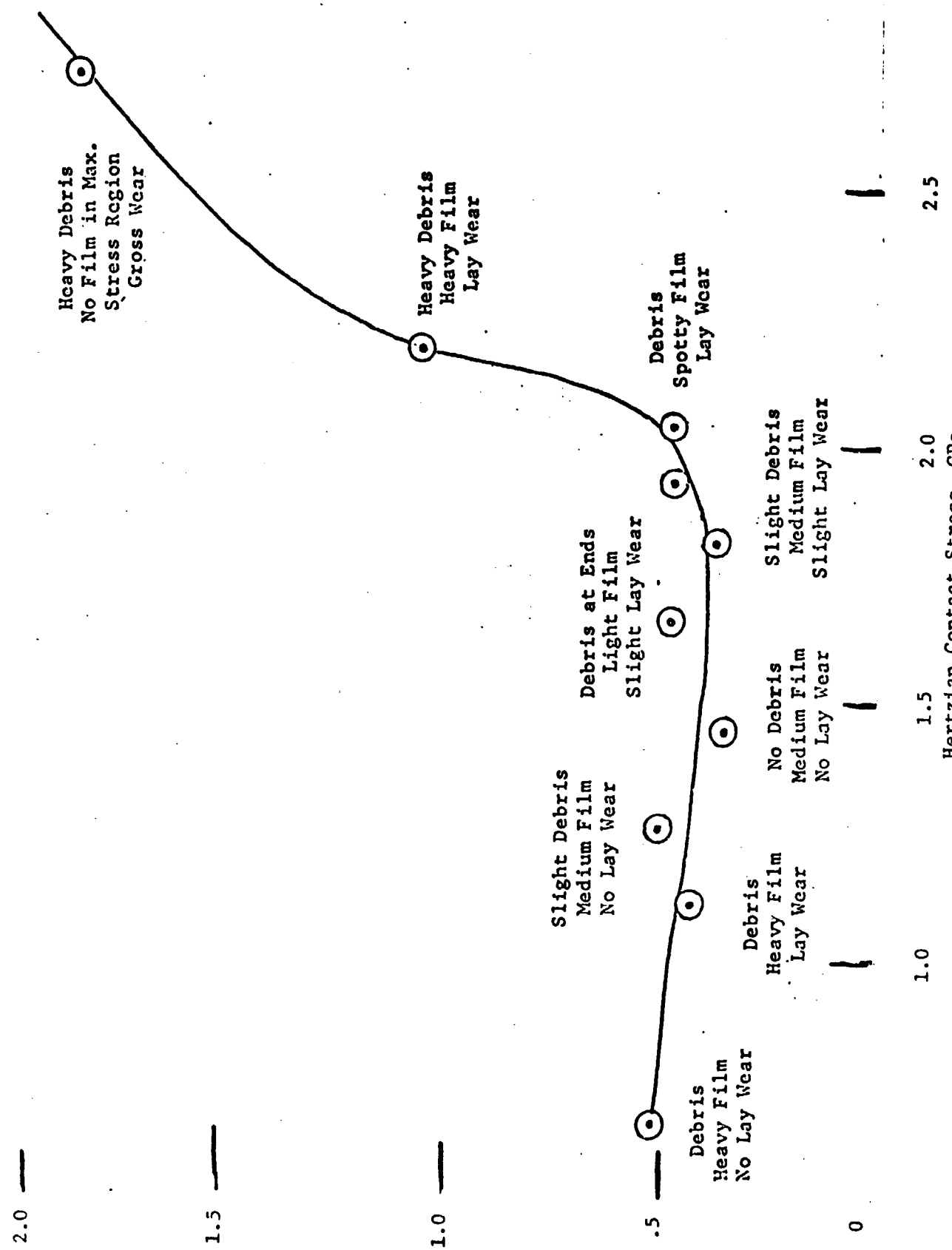

FIGURE 18. ADEQUACY OF TYPICAL TRANSFER FILM LUBRICANT

Measuring Units

Since the bearing drawings and all input data provided by NASA were in English units, all measurements and calculations were performed in English units. Therefore, the SI units presented in this report were converted from English units. Data on which this report is based are located in Battelle Laboratory Record Book No. 34405.